ASIAN JOURNAL OF CIVIL ENGINEERING (BUILDING AND HOUSING) VOL. 4, NOS 2-4 (2003)
PAGES 73-89

MODELLING OF THE DYNAMIC LOAD PLATE TEST WITH THE LIGHT FALLING WEIGHT DEVICE

C. Adam*
Institut fuer Allgemeine Mechanik, Vienna University of Technology
Wiedner Hauptstr. 8/E201, A-1040 Vienna, Austria, and
D. Adam
Institute for Ground Engineering and Soil Mechanics, Vienna University of Technology
Karlsplatz 13, A-1040 Vienna, Austria

ABSTRACT

In this paper mechanical modelling of the dynamic load plate test with the Light Falling Weight Device (LFWD) is presented. The LFWD is employed on construction sites to verify the compaction degree of soil layers and to evaluate their bearing capacity. The mechanical models developed are intended to provide simple and efficient formulations, which allow a large number of numerical simulations at low expenses. The motion of the device is characterized by a mass-spring-dashpot system. Several one-dimensional linear and nonlinear representations of the soil are discussed and evaluated. Different phases of motion of the LFWD - soil interaction system are identified, and corresponding formulations of the equations of motion are given. In appendices efficient solution procedures of the governing equations of motion are proposed.

Keywords: compaction control, device-soil interaction, motion dependent discontinuities, soil dynamics

1. INTRODUCTION

The Light Falling Weight Device (LFWD) is an innovative field test method, which provides the dynamic deformation modulus of soils and filled materials within earth structures and in ground engineering. The device is suitable to prove the compaction degree and to evaluate the bearing capacity of the tested soil layer. The dynamic load plate provides numerous advantages compared to the conventional static load plate. The LFWD is light and robust, and it can be carried and operated by a single person on the construction site. It allows measurements during the construction process, and it can also be used in narrow workspaces such as utility trenches. The simple operation of the device and the quick test implementation make a higher number of tests possible. Consequently, the quality control of the tested soil layers can be significantly improved.

* E-mail address of the corresponding author: ca@allmech9.tuwien.ac.at

In a comprehensive research project [1] conducted at the Institute for Ground Engineering and Soil Mechanics, Vienna University of Technology, the dynamic load plate test with the LFWD has been investigated. Parametric studies have been carried out in an effort to detect, understand, and explain phenomena arising in the field when the LFWD is applied. Results of large-scale in-situ tests at precisely defined soil conditions have been analyzed. Measured data of traditional and innovative compaction control methods (e.g. static load plate test, continuous compaction control) have been set in contrast with results from the dynamic load plate test. Technical prerequisites and demands regarding the device have been given. These studies are to be supplemented by outcomes from extensive numerical simulations. Therefore, in this paper simple mechanical models are described, which represent the main effects of the LFWD - soil interaction. The motion of the coupled LFWD - soil system can be characterized by a composition of linear springs, viscous dampers, and point masses. Applying a substructure technique both subsystems (LFWD and soil) are treated separately, and subsequently coupled stepwise by means of compatibility requirements. These models permit a careful dynamic analysis in order to optimize the performance of LFWD systems at low expenses.

2. CHARACTERIZATION OF THE LIGHT FALLING WEIGHT DEVICE (LFWD)

In Figure 1 a sketch of the LFWD is shown. During the field test with the LFWD an impact-like load is applied to the subsoil via a rigid circular steel plate (load plate). The load set consists of a falling weight and a guide rod. After release the falling weight slides down along the guide rod and hits a spring-damper element made of steel or synthetic material. In general the falling height is approximately 0.7 m. The rod rests on a sphere (without connection) in the middle of the load plate, and thus, only compression forces can be transferred onto the load plate. A sensor installed in the centre of the load plate records the acceleration, which subsequently renders the (maximum) plate displacement.

In a simplified procedure the average maximum plate displacement of three consecutive tests leads to an approximation of the dynamic deformation modulus of the tested soil layer. Thereby, the maximum soil contact stress is hypothetically assumed to be a constant, i.e. it is assumed to be independent from the soil type. Eventually, the dynamic deformation modulus can be related to the compaction degree of the tested soil layer. For details of the test evaluation see e.g. [2, 3].

According to German provisions [4] the main device parameters are standardized. In the following these parameters are briefly reviewed.

- Load plate:
  Radius 150 mm, thickness 20 mm, mass 15 kg
- Load set:
  mass of falling weight 10 kg, mass of guide rod 5 kg, maximum impact force 7.07

kN, impact duration 18 ms +(-) 2 ms

- Measuring instruments:
  Frequency range 8 - 100 Hz, displacement amplitude 0.2 - 1.0 mm: accuracy 0.02
  mm, 1.0 - 2.0 mm: accuracy 2%

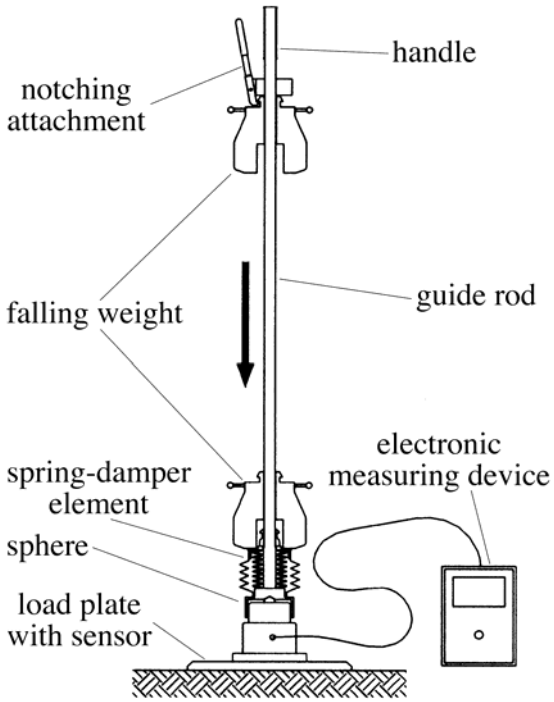

Figure 1. Components of the Light Falling Weight Device (LFWD)

3. MECHANICAL MODELING OF THE LFWD

In an approximation the LFWD may be characterized as a spring-dashpot-mass system, as shown in Figure 2. The point mass, which rests on the soil, accounts for the mass m_p of the load plate and the mass m_s of the guide rod. The mechanical properties of the spring-damper element are modelled as a Kelvin-Voigt body, i.e. a linear spring with stiffness k, and a viscous damper with damping coefficient c, Ref. [2]. Depending on the artefact of the LFWD the spring may be precompressed (denoted by z_{0pre}). The viscoelastic spring - damper element connects the point mass resting on the soil and a weightless top plate. F denotes the soil contact force. The falling weight is represented by the point mass m and it impacts upon the top plate after its release from the height h_0. It is noted that friction between the falling weight and the guide rod can be

neglected.

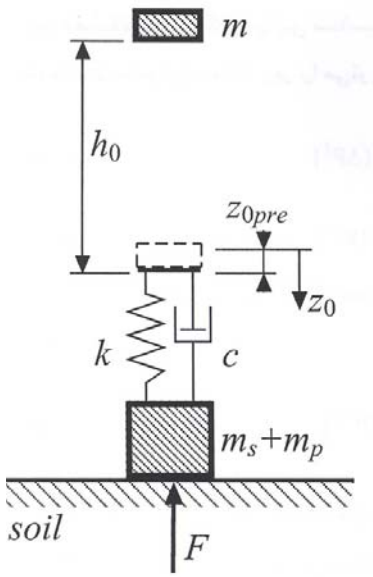

Figure 2. Mechanical model of the LFWD

4. MECHANICAL MODELING OF THE SOIL

The dynamic response of the soil can be calculated rigorously based on three-dimensional continuum mechanics with numerical methods such as the boundary-element or the finite-element method. These procedures are computationally expensive and belong more to the discipline of applied computational mechanics. Because the aim of this investigation is rather to understand (examine) the interaction system of soil - LFWD than to carry out a detailed investigation of the processes in the soil it seems to be appropriate to focus on simplified mechanical models, which reflect the main phenomena occurring during application of the load plate test with the LFWD. Besides their simple configuration these simplified soil models allow for a large number of timesaving simulations at low expenses.

4.1 Viscoelastic soil modeling

The LFWD is applied for testing the load-deformation behaviour of well-compacted soil layers, whereas the compaction of the soil itself represents a significant non-linear process. Thus, for the test with the LFWD the soil may be considered in a first approach to be a homogenous ideal elastic medium. Wolf and co-workers (see e.g. [5, 6]) have developed in a series of publications a simple viscoelastic model, where the soil is idealized as a semi-infinite truncated cone. For the current investigation the approach of Wolf is adopted. In this idealization the complex dynamic soil behaviour is reduced to a viscoelastic one-dimensional wave propagation problem, which can be represented by an equivalent frequency independent spring-mass-dashpot system, see Figure 3.

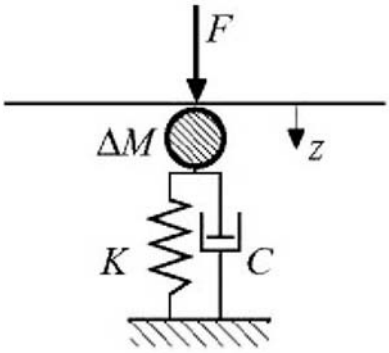

Figure 3. One-dimensional soil model of the elastic homogeneous halfspace

This model is only capable to simulate the soil reaction on the load plate; dynamic processes in the half space cannot be investigated. The stiffness of the cone is denoted by the spring stiffness K, while the wave propagation into the subsoil is associated to the geometric damping coefficient C. For cohesive soils the derivation gives an additional mass ΔM, which is, however, small compared to the mass (m_s + m_p) of the loading device. The importance of material damping is of second order for the current interaction problem, and hence neglected [2]. Depending on the nature of the soil K, C and ΔM are determined from elastic soil characteristics such as the dynamic compression modulus E_{dyn}, Poisson's ratio ν and (moisture) density ρ, and from the geometry of the loading area, i.e. the radius r of the load plate. According to [5, 7] these relations are given by:

$$K = 2rE_{dyn}\frac{1-2\nu}{(1-\nu)^2} \text{ for non-cohesive } (\frac{1}{3} < \nu \le \frac{1}{2}) \text{ and cohesive soils } (\nu \le \frac{1}{3}) \tag{1}$$

$$C = \sqrt{2\rho E_{dyn}}r^2\pi \quad \text{for non-cohesive soils} \tag{2}$$

$$C = \sqrt{2\rho E_{dyn}\frac{1-2\nu}{1-\nu}}r^2\pi \quad \text{for cohesive soils} \tag{3}$$

$$\Delta M = 2.4\pi\left(\nu - \frac{1}{3}\right)\rho r^3 \quad \text{for cohesive soils} \tag{4a}$$

$$\Delta M = 0 \text{ for non-cohesive soils} \tag{4b}$$

The equivalent stiffness K for cohesive and non-cohesive soils is identical, whereas the viscous damping coefficients differ for both types of soil.

Previous studies (e.g. [5, 6, 7]) based on cone models have shown that they provide

conceptual clarity with physical insight, simplicity, and sufficient generality, although they do lead to some loss of accuracy. The accuracy of any analysis is limited anyway because of many uncertainties such as those linked to dynamic soil properties, some of which can never be eliminated.

4.2 Consideration of varying loading/unloading soil stiffness

Successive repetition of the dynamic load test on the same spot leads to an increasing deformation modulus even for well-compacted soil, i.e. the stiffness of the soil increases with each impact. At the same time permanent deformation of the loaded surface can be observed. The reason is that dynamic impact loading induces consolidation of the soil by reduction of its pore volume. However, for compacted soil the additional permanent (plastic) portion is small compared to the reversible (elastic) portion. These effects may be accounted to the fact that the stiffness of the soil depends on the direction of load. In general, the soil behaves stiffer when unloaded.

For a more thorough investigation of the soil - LFWD interaction it is desirable to consider this behaviour in the soil model. In a first-order approach the loading and unloading branch of deformation may be approximated by a piecewise linear function, coming up with a so-called saw tooth model (see Figure 4).

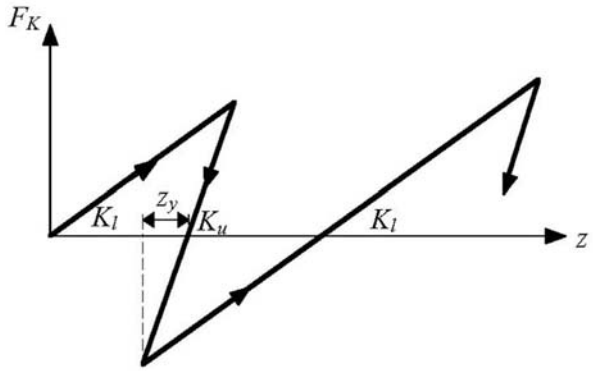

Figure 4. Characteristics of the soil spring considering different loading and unloading stiffness (saw tooth model)

The saw tooth model leads to plastic deformation in one direction at cyclic loading. During the transition from loading to unloading and vice versa the plastic deformation is modified according to a Heaviside function. Compatibility requires that the force in the spring does not exhibit a jump at the reversal from unloading to loading (and vice versa). According to Hooke's law [8] this condition may be expressed as:

$$F_k = K_l \left(z_y - z_l^{pl} \right) \equiv K_u \left(z_y - z_u^{pl} \right) \tag{5}$$

In equation (5) z_l^{pl} and z_u^{pl}, respectively, represent the portions of plastic deformation in the loading and unloading period. K_l and K_u denote the spring stiffness during loading and unloading, respectively. For an explanation of F_k, z_y see Figure 4. At the instant of transition

from unloading to loading equation (5) can be solved for z_u^{pl} :

$$z_u^{pl} = \left(1 - \frac{K_l}{K_u}\right) z_y + \frac{K_l}{K_u} z_l^{pl} \tag{6}$$

Contrary, z_l^{pl} can be derived as:

$$z_l^{pl} = \left(1 - \frac{K_u}{K_l}\right) z_y + \frac{K_u}{K_l} z_u^{pl} \tag{7}$$

During periods of loading/unloading the plastic deformation is a constant.

Note that the soil parameters such as stiffness and damping coefficients are still governed by equations (1 - 4), however, modulus E_{dyn} is now a function of the loading direction. Hence, it is more appropriate to write $E_{dyn,l}$ for loading and $E_{dyn,u}$ for unloading. Inspection of equations (2) and (3) reveals that also the damping coefficients depend on the loading direction because the are derived among other parameters from $E_{dyn,l}$ and $E_{dyn,u}$, respectively.

However, it should be mentioned that for the evaluation of the dynamic deformation modulus after a standard test only the loading phase of the first impact is considered.

4.3 Detailed modelling of the loading area

In the near field of the load plate the soil is exposed to large stresses and strains, and hence, it experiences plastic deformations. However, the far field of the soil remains elastic during the entire dynamic process. Thus, a separate consideration of the near field and the far field seems to be reasonable. In a simplified assumption the near field the of soil is modelled by an additional soil spring K_p. This spring is in series with the spring-damper element of the viscoelastic soil model, determined from the cone theory, see Figure 5. The stiffness K_p of the additional spring can be estimated by relating the maximum applied load $P_{\max}$, and the permanent deformation z^{pl} from a static load test:

$$K_P = \frac{P_{\max}}{z^{pl}} \tag{8}$$

For well compacted soils the stiffness K_p will be in any case larger than the stiffness K of the spring, which simulates the elastic half space.

According to the cone theory the additional soil mass ΔM (for cohesive soils) is assigned to the top of the upper soil spring.

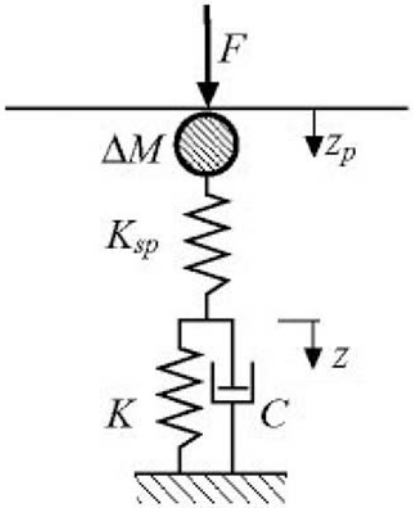

Figure 5. Soil modelling of the loading area by an additional soil spring

5. EQUATIONS OF MOTION OF THE LFWD-SOIL INTERACTION SYSTEM

The mechanical models of the both subsystems LFWD and soil are coupled by means of the substructure technique and application of the compatibility requirements. Mechanically the motion of the interaction system can be classified as a system with motion dependent discontinuities. In the following considerations the sequence of the different phases of motion are identified, and the corresponding mathematical equations are specified. It is noted that soil and load plate are assumed to be connected during the entire motion. Hence, the mass of the load plate m_p, the mass of the guide rod m_s, and the equivalent soil mass ΔM can be combined to a single point mass M:

$$M = m_s + m_p + \Delta M \tag{9}$$

5.1 Viscoelastic soil model

Subsequently, the motion of the LFWD and the viscoelastic soil model according to section 4.1 is considered, see Figure 6. The displacement of the mass m is denoted by z_0, whereas the coordinate z is assigned to equivalent mass M. The spring of the load plate is assumed to be precompressed by z_{0pre}. *The* following phases of motion can be identified.

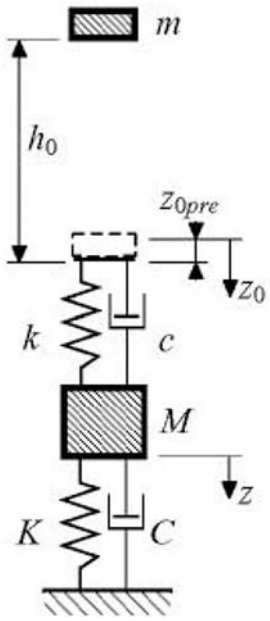

Figure 6. Mechanical modelling of the dynamic interaction system LFWD - elastic soil

Phase 1: fall phase
At time instant t_0 (t = 0) the mass m is released and it falls from the height h_0 through the loading device. The initial conditions of the masses m and M can be expressed as:

$$z_0\left(t_0\right) = -h_0 + z_{0\,pre} \;,\; z\left(t_0\right) = 0 \tag{10}$$

During the fall ($t_0 \le t \le t_1$) the displacement and the rate of fall of the mass m are given by

$$z_0 = g\frac{t^2}{2} - h_0 + z_{0\,pre} \;,\; \dot{z}_0 = gt \tag{11}$$

While the load plate is at rest,

$$z = \dot{z} = 0 \tag{12}$$

In (11) g denotes the acceleration of gravity. At time instant t_1,

$$t_1 = \sqrt{\frac{2h_0}{g}} \tag{13}$$

the mass m hits the weight-less top plate of the load plate model, and subsequently, mass m, load plate and soil are in full contact.

Phase 2: full contact phase

In the full contact phase the behaviour of the model is governed by a coupled system of differential equations with two-degree-of freedoms (2DOF):

$$\begin{bmatrix} m & 0 \\ 0 & M \end{bmatrix} \begin{Bmatrix} \ddot{z}_0 \\ \ddot{z} \end{Bmatrix} + \begin{bmatrix} c & -c \\ -c & c+C \end{bmatrix} \begin{Bmatrix} \dot{z}_0 \\ \dot{z} \end{Bmatrix} + \begin{bmatrix} k & -k \\ -k & k+K \end{bmatrix} \begin{Bmatrix} z_0 \\ z \end{Bmatrix} = \begin{Bmatrix} mg \\ 0 \end{Bmatrix} \tag{14}$$

The initial conditions are defined by equations (11, 12) at time instant t_1. Note that the spring of the soil is already precompressed by the dead weight Mg, and consequently Mg does not show up on the right hand side of equations (14).

As long as the conditions

$$-kz_{0\,pre} + k\left(z - z_0\right) + c\left(\dot{z} - \dot{z}_0\right) \le 0 \quad \text{and} \quad z_0 - z_{0\,pre} \ge z \tag{15}$$

are satisfied mass m and the load device are in full contact. A proper solution procedure of equations (14) is given in Appendix A1.

Phase 3: uplift phase

At time instant t_2 the mass m lifts up from the load plate, and during a standard test on the construction site investigate also the subsequent motion of the system.

In test devices with a pre-compressed spring K two different conditions of incipient uplift do exist. These conditions are defined as follows:

- the force in the spring-damper element is zero:

$$-kz_{0\,pre} + k\left(z - z_0\right) + c\left(\dot{z} - \dot{z}_0\right) = 0 \tag{16}$$

- the spring cannot expand beyond its pre-compressed length, i.e. the spring deflection corresponds to its initial value at time instant t_1:

$$z_0 - z_{0\,pre} = z \tag{17}$$

The condition, which occurs at first, is relevant for uplift.

In the uplift phase the motion of the mass m is determined by the gravity and the initial conditions at $t = t_2$: $z_0(t_2)$, $\dot{z}_0\left(t_2\right)$:

$$z_0 = g\frac{(t-t_2)^2}{2} + z_0(t_2) + \dot{z}_0(t_2)(t-t_2)\ , \quad \dot{z}_0 = g(t-t_2) + \dot{z}_0(t_2) \tag{18}$$

The load plate, which is according to observations in contact to the soil during the entire test procedure, is in phase 3 in free vibration and its displacement z is governed by the homogenous differential equation of motion

$$M\ddot{z} + C\dot{z} + Kz = 0 \tag{19}$$

and the initial conditions $z(t_2)$ and $\dot{z}(t_2)$.

During the test the guide rod lifts up from the load plate because only force in compression can be transferred between both components of the test device. However, this time-instant is insignificant for the mechanical simulation of the test, and subsequently, during this short period of time accurate modelling of this effect may be disregarded. When the mass m impacts the load plate the second time it can be assumed that guide rod, load plate and soil are already at rest. Furthermore, the spring-damper element is supposed to be at its initial position.

Phase 4: re-contact phase
The time instant t_3 of the second impact is derived from the time period of uplift of the mass m:

$$t_3 = \sqrt{\frac{2\left[h_r + z_0(t_2) + z(t_2)\right]}{g}} + \sqrt{\frac{2h_r}{g}} + t_2 \approx \sqrt{\frac{8h_r}{g}} + t_2 \tag{20}$$

In (20) h_r denotes the rebound height. The subsequent motion of the coupled system is described in analogy to phase 2 by equations (14). The corresponding initial conditions are defined by $z_0(t_3)$, $\dot{z}_0(t_3)$ and $z(t_3) = \dot{z}(t_3) = 0$, respectively.

5.2 Consideration of varying loading/unloading soil stiffness
Here, the soil model of section 4.2 according to a saw tooth is utilized, see Figure 4. The phases of discontinuous motion identified in the previous section remain the same, however, in phases 2, 3 and 4 the equations of motion are to be subdivided in periods of loading and unloading. On the left hand side damping and stiffness coefficients of the soil are replaced by load direction dependent coefficients, the plastic portion of deformation is considered as additional (so called internal) loading, and thus, written on the right hand side [12].

Phases 2 and 4: full contact and re-contact phase, respectively
The equations of motion (14) are to be separated in periods of loading and unloading, and may be written as follows,

$$\begin{bmatrix} m & 0 \\ 0 & M \end{bmatrix}\begin{Bmatrix} \ddot{z}_0 \\ \ddot{z} \end{Bmatrix} + \begin{bmatrix} c & -c \\ -c & c + C_i \end{bmatrix}\begin{Bmatrix} \dot{z}_0 \\ \dot{z} \end{Bmatrix} + \begin{bmatrix} k & -k \\ -k & k + K_i \end{bmatrix}\begin{Bmatrix} z_0 \\ z \end{Bmatrix} = \begin{Bmatrix} mg \\ K_i z_i^{pl} \end{Bmatrix},\ i = l,\ u \tag{21}$$

where subscript $i = l$ denotes the sub phase loading, whereas $i = u$ indicates the sub phase unloading. During the transition from loading and unloading not only the modal properties (i.e. natural frequencies, modal damping coefficients and mode shapes) of the coupled system vary but also the plastic part of deformation according to equations (6) or (7).

Phase 3: uplift phase
In the uplift phase it is differentiated between the sub phases loading and unloading as well:

$$M\ddot{z} + C\dot{z} + Kz = K_i z_i^{pl} \quad , i = l, u \tag{22}$$

5.3 Consideration of detailed modelling of the soil in the loading area
Taking into account inelastic soil behaviour of the loading area according to section 4.3 an additional degree of freedom characterizes the motion of the soil. This additional degree of freedom is denoted by z_p, see Figure 7. Only load devices without precompressed springs are considered in the actual formulation. For numerical investigations performed the ratio of ε_k of both soil springs is utilized:

$$\varepsilon_k = \frac{K_p}{K} \tag{23}$$

All phases of motion identified in section 5.1 apply; however, differences in the formulation of the equations of motion are subsequently outlined.

Phase 1: fall phase
The soil is at rest, and hence, equations (10 - 13) are still valid (with $z_{0pre} = 0$). In addition, displacement and rate of the additional degree of freedom are also zero:

$$z_P = \dot{z}_P = 0 \tag{24}$$

Phase 2: full contact phase
The dynamics of the system in full contact is described by a coupled set of three equations of motion, which may be written as

$$\begin{bmatrix} m & 0 & 0 \\ 0 & M & 0 \\ 0 & 0 & 0 \end{bmatrix} \begin{Bmatrix} \ddot{z}_0 \\ \ddot{z}_p \\ \ddot{z} \end{Bmatrix} + \begin{bmatrix} c & -c & 0 \\ -c & c & 0 \\ 0 & 0 & C \end{bmatrix} \begin{Bmatrix} \dot{z}_0 \\ \dot{z}_p \\ \dot{z} \end{Bmatrix} + \begin{bmatrix} k & -k & 0 \\ -k & k+K_p & -K_p \\ 0 & -K_p & K_p+K \end{bmatrix} \begin{Bmatrix} z_0 \\ z_p \\ z \end{Bmatrix} = \begin{Bmatrix} mg \\ 0 \\ 0 \end{Bmatrix} \tag{25}$$

The dead weight of mass M does not enter the above equations because both soil springs are already pre-compressed by it. At time instant t_1, the vibration of the system is initialized by the velocity of the mass m: $\dot{z}_0(t_1)$, all other initial conditions are zero. In Appendix A2 a proper solution procedure is examined.

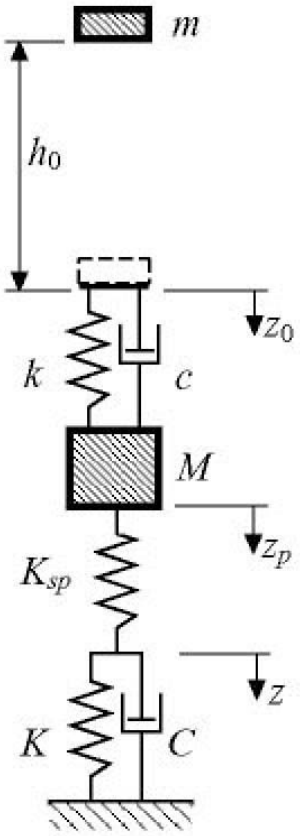

Figure 7. Mechanical modeling of the dynamic interaction system LFWD - soil. Detailed modeling of the loading area

Phase 3: uplift phase

The condition of uplift is determined by condition (16) with $z_{0pre} = 0$. In the subsequent phase the motion of the coupled load plate - soil model is given by following equations:

$$\begin{bmatrix} M & 0 \\ 0 & 0 \end{bmatrix} \begin{Bmatrix} \ddot{z}_p \\ \ddot{z} \end{Bmatrix} + \begin{bmatrix} 0 & 0 \\ 0 & C \end{bmatrix} \begin{Bmatrix} \dot{z}_p \\ \dot{z} \end{Bmatrix} + \begin{bmatrix} K_p & -K_p \\ -K_p & K_p + K \end{bmatrix} \begin{Bmatrix} z_p \\ z \end{Bmatrix} = \begin{Bmatrix} 0 \\ 0 \end{Bmatrix} \tag{26}$$

For this type of coupled equations with only one dynamic active mass the corresponding initial conditions are $z_p(t_2)$, $\dot{z}_p(t_2)$, $z(t_2)$. Equations (26) can be solved by application of a similar approach as described in Appendix A2 [2].

For the displacement and velocity of the mass *m* expressions (18) hold.

Phase 4: re-contact phase
In this phase the same equations as in phase 2 are employed. The time instant t_3 of impact is determined by:

$$t_3 = \sqrt{\frac{2\left[h_r + z_0(t_2) + z_p(t_2) + z(t_2)\right]}{g}} + \sqrt{\frac{2h_r}{g}} + t_2 \approx \sqrt{\frac{8h_r}{g}} + t_2 \qquad (27)$$

It is assumed that load plate and soil are at rest, and hence, all initial conditions besides $\dot{z}_0(t_3)$ are zero.

6. CONCLUSIONS

Different mechanical models for the simulation of dynamic load test with the Light Falling Weight Device (LFWD) have been presented in an effort to provide efficient numerical algorithms. Depending on the effects to be investigated the tested soil has been characterized by means of one-dimensional representations of the half space. Viscoelastic models with varying loading and unloading stiffness and with detailed modelling of the loading area have been considered. Different phases of discontinued motion have been identified and described by mathematical equations. It is noted that comparative studies of measured and simulated data can be found in [1, 2, 3, 9].

Acknowledgment: The support of C. Adam in his research at Stanford University by a fellowship of the *Max Kade Foundation, Inc.* is gratefully acknowledged.

REFERENCES

1. Brandl, H., Adam, D., Kopf, F. and Niederbrucker, R., "*The dynamic load plate test with the Light Falling Weight Device"* (in German). Bundesministerium fuer Verkehr, Innovation und Technologie, Vienna, Strassenforschung 528, 2003.
2. Müller, C., "*The Light Falling Weight Device. A new and innovative compaction testing method. Theory and practice"* Master's Thesis, Vienna University of Technology, 2003.
3. Adam, D., Adam, C. and Kopf, F., "The dynamic load plate test with the Light Falling Weight Device: Experimental and numerical investigations". In: *Proceedings 11th International Conference on Soil Dynamics and Earthquake Engineering* (11th *ICSDEE*), 7th - 9th January 2004, University of California, Berkeley, Vol 1, pp. 649-654. Stallion Press, 2004.
4. *Technical test provisions for soil and rock in road constructions TP BF - StB, part B 8.3: Dynamic plate compression test with the Light Falling Weight Device* (in

German). Cologne: Forschungsgesellschaft fuer Strassen- und Verkehrswesen 2003.
5. Wolf, J.P., "*Foundation analysis using simple physical models"*, Prentice-Hall, Englewood Cliffs, N.J., 1994.
6. Wolf, J.P. and Preisig, M., "Dynamic stiffness of foundation embedded in layered half space based on wave propagation in cones", *Earthquake Engineering and Structural Dynamics*, **32**(2003) 1075-1098.
7. Adam, D., *"Continuous compaction control (CCC) with vibratory rollers* (in German), Doctoral thesis, Vienna University of Technology, 1996.
8. Ziegler, F., "*Mechanics of solids and fluids*, 2nd reprint of the 2nd edition", Springer, New York, 1998.
9. Adam, D., Kopf, F. and Adam C., "The dynamic load plate test with the Light Falling Weight Device-Theoretical and experimental investigations (in German)", *Der Bauingenieur*, **79**(2004) 1185-1192.
10. Holl, H.J., "A time integration algorithm for time-varying systems with non-classical damping based on modal methods". In: Wicks, A.L. (ed.) *Proceedings* 15*th IMAC*, 1997, Orlando, pp. 1558-1564.
11. Raue, A. and Ziegler, F., "Modal analysis of non classically damped structures". In: Guidati, G., Heller, H., Heiss, A. (eds) *Proceedings* 7*th International Congress on Sound and Vibration* (*ICSV* 7), 2000, Garmisch Partenkirchen, pp. 829-836, Kramer Technology Publishing, Munich 2000.
12. Adam, C. and Fotiu, P.A., "Dynamic analysis of inelastic primary-secondary systems", *Engineering Structures*, **22**(2000) 58-71.
13. Chopra, A.K., "*Dynamics of Structures"*, Prentice-Hall, Englewood Cliffs, N.J., 1995.

APPENDIX A1

The solution of the coupled set of differential equations (14) is composed of a time invariant static portion (denoted by superscript *S*) and a dynamic portion (denoted by a superscript *D*),

$$z_0 = z_0^S + z_0^D \ , \ \ z = z^S + z^D \tag{A1}$$

with

$$\dot{z}_0^S = \ddot{z}_0^S \equiv 0 \ , \ \ \dot{z}^S = \ddot{z}^S \equiv 0 \tag{A2}$$

The static displacements of the 2DOF system are derived from the relations

$$z_0^S = mg\left(\frac{1}{k} + \frac{1}{K}\right) \ , \ \ z^S = \frac{mg}{K} \tag{A3}$$

whereas the complementary dynamic response represented by the 2DOF set of differential equations,

$$\begin{bmatrix} m & 0 \\ 0 & M \end{bmatrix} \begin{Bmatrix} \ddot{z}_0^D \\ \ddot{z}^D \end{Bmatrix} + \begin{bmatrix} c & -c \\ -c & c+C \end{bmatrix} \begin{Bmatrix} \dot{z}_0^D \\ \dot{z}^D \end{Bmatrix} + \begin{bmatrix} k & -k \\ -k & k+K \end{bmatrix} \begin{Bmatrix} z_0^D \\ z^D \end{Bmatrix} = \begin{Bmatrix} 0 \\ 0 \end{Bmatrix} \tag{A4}$$

is induced by the initial conditions at time instant t_1:

$$z_0^D(t_1) = -z_0^S + z_{0\,pre} \;,\; \dot{z}_0^D(t_1) = \dot{z}_0(t_1) \;,\; z^D(t_1) = -z^S \;,\; \dot{z}^D(t_1) = 0 \tag{A5}$$

Equations (A4) are solved by modal decomposition of the geometric coordinates:

$$\begin{Bmatrix} z_0^D \\ z^D \end{Bmatrix} = \begin{bmatrix} \phi_{11} & \phi_{12} \\ \phi_{21} & \phi_{22} \end{bmatrix} \begin{Bmatrix} Y_1 \\ Y_2 \end{Bmatrix} \tag{A6}$$

where ϕ_{ik} are the coefficients of the mode shapes of the *undamped* system. Because equations (A4) are non-proportional damped the modal equations are coupled via non-diagonal modal damping coefficients. These equations are formally decoupled by considering the non-diagonal terms as fictitious loading, see e.g. Holl [10], Raue and Ziegler [11]:

$$m_i^* \ddot{Y}_i + c_{ii}^* \dot{Y}_i + k_i^* Y_i = P_i^* \;,\; P_i^* = -c_{ik}^* \dot{Y}_k \;,\; i=1,\; k=2 \;,\; i=2,\; k=1 \tag{A7}$$

where m_1^*, m_2^* are the modal masses, k_1^*, k_2^* denote the modal stiffness, and c_{11}^*, c_{22}^* and c_{12}^*, c_{21}^* represent the diagonal and the off-diagonal damping terms, respectively, in the modal space (see e.g. [11, 12]). This formulation provides two equations of the linear SDOF oscillator, and thus, linear solution methods such as Duhamel's integral can be applied, see e.g. Chopra [13]. The fictitious loadings P_i^*, however, are not known in advance, which necessitates an iterative time-stepping procedure to solve equations (A7).

The initial conditions must also be converted in modal coordinates, e.g. the modal displacements at time instant t_1 are given as:

$$Y_2(t_1) = \frac{z_0^D(t_1)\phi_{21} - z^D(t_1)\phi_{11}}{\phi_{12}\phi_{21} - \phi_{11}\phi_{22}} \;,\; Y_1(t_1) = \frac{z_0^D(t_1) - Y_2(t_1)\phi_{12}}{\phi_{11}} \tag{A8}$$

Subsequently, the accelerations are found by solving equations (14) for $\ddot{z}_0$ and $\ddot{z}$.

APPENDIX A2

Here, the solution of the coupled set of equations of motion (25) is discussed. As already shown in Appendix A1 for a 2DOF system the geometric coordinates are separated in a static and complementary dynamic portion. For the displacements z_0 and z relations (A1) and (A2) apply, the additional coordinate z_p is supplemented by,

$$z_p = z_p^S + z_p^D \,, \quad \dot{z}_p^S = \ddot{z}_p^S \equiv 0 \tag{A9}$$

The quasistatic portion of the response is determined by,

$$z_0^S = mg\left(\frac{1}{k} + \frac{K + K_p}{KK_p}\right) \,, \quad z_P^S = mg\frac{K + K_p}{KK_p} \,, \quad z^S = \frac{mg}{K} \tag{A10}$$

the complementary dynamic response is found from the following coupled set of three differential equations,

$$\begin{bmatrix} m & 0 \\ 0 & M \end{bmatrix}\begin{Bmatrix} \ddot{z}_0^D \\ \ddot{z}_p^D \end{Bmatrix} + \begin{bmatrix} c & -c \\ -c & c \end{bmatrix}\begin{Bmatrix} \dot{z}_0^D \\ \dot{z}_p^D \end{Bmatrix} + \begin{bmatrix} k & -k \\ -k & k + K_p \end{bmatrix}\begin{Bmatrix} z_0^D \\ z_p^D \end{Bmatrix} = \begin{Bmatrix} 0 \\ K_p z^D \end{Bmatrix} \tag{A11.1}$$

$$C\dot{z}^D + \left(K + K_p\right)z^D = K_p z_p^D \tag{A11.2}$$

and the corresponding initial conditions,

$$z_0^D\left(t_1\right) = -z_0^S \,, \; \dot{z}_0^D\left(t_1\right) = \dot{z}_0\left(t_1\right) \,, \; z_p^D\left(t_1\right) = -z_p^S \,, \; \dot{z}_p^D\left(t_1\right) = 0 \,, \; z^D\left(t_1\right) = -z^S \tag{A12}$$

Equations (A11) are written as a 2DOF system and a first order differential equation, the coupling terms are written on the right hand side. These equations are solved by means of a substructure technique, where the coupling terms are treated as additional forces acting on the corresponding subsystem [12].